RSC Advances

PAPER

View Article Online
View Journal | View Issue

Cite this: *RSC Adv.*, 2022, **12**, 7941

Selective preconcentration separation of Hg(II) and Cd(II) from water, fish muscles, and cucumber samples using recycled aluminum adsorbents†

A. B. Abdallah, *[a] Ehab A. Abdelrahman,[b] Adel M. Youins, [a] Wesam A. Ibrahim[a] and Magdi E. Khalifa[a]

Received 3rd January 2022
Accepted 26th February 2022

DOI: 10.1039/d2ra00028h

rsc.li/rsc-advances

Modified aluminum scrap waste was used in the selective extraction of Hg(II), and Cd(II) ions. The aluminum scraps were modified with dibenzoylmethane, or isatoic anhydride, or 5-(2-chloroacetamide)-2-hydroxybenzoic acid. The modified aluminum sorbents were characterized by FT-IR, SEM, XRD, XPS, TGA, and elemental analysis. Modes of chelation between adsorbents and target metal ions were deduced *via* DFT. The highest adsorption capacity was observed for benzo-amino aluminum (BAA) toward Hg(II), which reached 234.56 mg g^{-1}, while other modified sorbents ranged from 135.28 mg g^{-1} to 229.3 mg g^{-1}. Under the optimized conditions, the BAA adsorbent showed a lower limit of detection (1.1 mg L^{-1}) and limit of quantification (3.66 mg L^{-1}) for mercury ions than other sorbents. The prepared aluminum adsorbents also exhibited significant selectivities for Hg(II) and Cd(II) ions in the presence of competing metal ions.

1. Introduction

In the last few decades, the global demand for Al (*e.g.* food plates, gutters, foil, soft drink cans, *etc.*) has seen significant growth due to its good formability, high strength and corrosion resistance.[1–3] Therefore, for environmental and economic benefits, the recycling of aluminum scrap is considered as a waste management process and has also produced several useful commercial products. The recycled aluminum, especially from aluminum cans are fit for further applications including the manufacturing of paperclips and ship hulls, and extraction of various pollutants.[2,3] For the adsorption of heavy metals from aqueous systems, the chemical and/or physical modification of aluminum scrap using certain organic materials including functional groups (*e.g.*, carboxylic group, amine group, hydroxyl group, *etc.*) is expected to enhance their sorption process.[4–6] The binding of an organic coating material to the surface of the recycled aluminum occurs by mixing the organic solution with the target adsorbent for a specific time. The solvent was allowed to evaporate, followed by air-drying to obtain the resultant adsorbent. Depending on their adsorbent modification, the removal mechanism of different metals is suggested. The target metal ions are not only extracted by adsorption on the modified alumina surface but also by surface attraction, in which chemical-bonding interactions occur between the newly added chemicals and the target heavy metal ions.

With the fast development of industry, heavy metal ions (*e.g.*, Hg(II), Cd(II), Pb(II), *etc.*) have been considered as a substantial issue due to their collection and expansion in various biological chains.[7,8] Although these metals are essential for different living organisms, they may cause harmful health problems at certain threshold concentrations. Thus, there is a critical need for a development method for the accurate determination of trace amounts of these heavy metals. Atomic absorption spectrophotometry, capillary electrophoresis, inductively coupled plasma, flame atomic fluorescence spectrometry, and electrochemical techniques are the most frequently used methods for the determination of these metals in different real samples.[9–12] Unfortunately, the accurate determination of these metal ions in environmental samples is still a difficult task owing to their low concentrations and the dominant effect of matrix components from the diverse ions. To overcome these limitations, preliminary separation and preconcentration processes become urgent steps that are needed before the direct measurement, especially in the presence of low concentrations of target ions. To date, numerous methods including solid phase extraction (SPE),[13–18] cloud point extraction (CPE),[19] flotation,[20] and liquid–liquid extraction (LLE)[21] have been designed for the separation and/or preconcentration of the heavy metal ions. Due to the high extraction efficiency, and rapid phase separation, the SPE has been widely applied as the preconcentration technique.[22–24] Based on these approaches, we report a simple and efficient synthetic method for recycling aluminum scrap, especially from aluminum cans. These adsorbents showed enhanced

[a]*Department of Chemistry, Faculty of Science, Mansoura University, El-Gomhoria Street, Mansoura 35516, Egypt. E-mail: ahmed.bahgat@mans.edu.eg*

[b]*Chemistry Department, Faculty of Science, Benha University, Benha 13518, Egypt*

† Electronic supplementary information (ESI) available. See DOI: 10.1039/d2ra00028h

performance for the separation and preconcentration of the target heavy metal ions (Hg(II), and Cd(II)) by modification with the promising chelating agents including dibenzoylmethane, isatoic anhydride and 5-(2-chloroacetamide)-2-hydroxybenzoic acid. The modified aluminum adsorbents were characterized by using Fourier transform infrared spectroscopy (FT-IR), X-ray diffraction (XRD), scanning electron microscopy (SEM), X-ray photoelectron spectroscopy (XPS), thermal gravimetric analysis (TGA), and elemental analysis. The selective extraction of Hg(II), and Cd(II) was optimized in detail prior to its determination by flame atomic absorption spectrometry (FAAS) and inductively coupled plasma optical emission spectroscopy (ICP-OES). The developed technique was validated for the studied metal ions and found to be robust and highly sensitive to low limits of detection for these heavy metal ions. Finally, these aluminum adsorbents were applied in the determination of the target ions in different real samples (*e.g.*, water samples, fish samples, and vegetable samples).

2. Experimental section

2.1. Chemicals and reagents

The aluminum cans were obtained from commercial shops (Mansoura, Egypt). Isatoic anhydride, dibenzoylmethane, 4-amino-2-hydroxy benzoic acid, toluene, cadmium(II) chloride, chloroacetyl chloride, nickel(II) chloride hexahydrate, ethylenediaminetetraacetic acid tetrasodium salt dihydrate, zinc(II) chloride, aluminum(III) chloride hexahydrate, iron(III) chloride hexahydrate, and lead(II) chloride were obtained from Sigma-Aldrich. Hydrochloric acid, potassium chloride, sodium hydroxide, mercury(II) chloride, and copper(II) chloride dihydrate were purchased from Merck (Germany). The other chemicals were of analytical grade, obtained from Fluka (Switzerland) and were used without further purification unless otherwise stated. In addition, all aqueous solutions in this work were prepared by using doubly distilled water (resistance: 18.2 MΩ at 25 °C). It is worth mentioning that all glassware was rinsed in concentrated nitric acid solution (1% (v/v)) and washed with doubly distilled water before use. For analytical applications, the cucumber, lettuce leaves, and wastewater samples were collected from different agricultural locations in Samanoud (El-Gharbia).

2.2. Instruments

The determination of metal contents was carried out using Agilent's 5100 ICP-OES (Agilent Technologies. Melbourne, Australia), and FAAS (GBC Scientific Equipment USA LLC, Hampshire, IL). A digital pH meter (HI 8519; Hanna Instruments, Italy) equipped with a combined Ag/AgCl glass electrode was used for adjusting the concentration of hydrogen ions during the extraction processes. FT-IR spectra of the modified aluminum scrap were obtained using an infrared spectrometer (Nicolet iS 10, Nicolet Instrument Co., Madison, WI, USA) over the wavenumber range from 400 cm^{-1} to 4000 cm^{-1} using pressed KBr pellets. The morphologies and compositions of the constructed sorbents were determined *via* scanning electron microscopy (JEOL JEM-2100 lv (HRTEM), JEOL Ltd., Tokyo, Japan), and energy-dispersive X-ray spectroscopy (X-Max 20, Oxford Instruments, UK), using an accelerating voltage of 15 kV. The percentage of the elements (C, H, N, S and O) in the ESI† was detected using a PerkinElmer 2400 CHN Elemental Analyzer (USA). The XPS spectra of the prepared sorbent before and after the adsorption of metal ions were obtained using a K-ALPHA instrument (Thermo Fisher Scientific, USA) with monochromatic X-ray Al K-alpha radiation −10 to 1350 eV and spot size of 400 μm at a pressure of 10^{-9} mbar. The TGA-DTG analysis was conducted for the modified sorbents at a heating rate of 10 °C min^{-1} in a N_2 atmosphere to examine the decomposition steps and thermal stabilities of the BAA, CAA and IAA ligands after the adsorption of Hg^{2+} and Cd^{2+} ions. The crystallinity of the solid particles was examined using a Bruker AXS diffractometer (Karlsruhe, Germany), 1.54056 Å wavelength, and Cu Kα X-ray source.

2.3. Preparation of aluminum scrap

Aluminum scrap was fabricated by a hydrothermal technique. Typically, 2 g of aluminum cans were dissolved in 50 mL of sodium hydroxide solution (2.5 M) after washing with boiled distilled water. Subsequently, 50 mL of sodium metasilicate pentahydrate solution, dissolved in sodium hydroxide solution, was added to the above mixture drop by drop with continuous stirring for 1 h at 850 rpm until homogenized. The produced gel was transferred into a stainless-steel autoclave and heated at 150 °C for 6 h. After that, the produced precipitate was washed several times with double distilled water and dried under vacuum for 12 h at 80 °C. Two grams of the aluminum powder precipitation was refluxed with 2.2 mL of (3-aminopropyl)trimethoxysilane in 30 mL toluene at 120–140 °C for 24 h. The resulting material was washed thoroughly with ethanol, dried at 50 °C for 24 h, ground and sieved to obtain the amino-derivative of the aluminum particles. In the subsequent reaction, the resultant amino aluminum powder (2 g) was refluxed again, for 24 h with 25 mL of ethanolic solution of dibenzoylmethane (0.36 M) in the presence of a few drops of sulfuric acid. After that, the product (benzo-amino aluminum (BAA)) was filtered, washed with ethanol, and dried at 60 °C for 12 h. Similarly, the derivative amino aluminum powder was reacted with isatoic anhydride reagent to produce the isa-amino aluminum sorbent (IAA). To produce the chloro-amino aluminum adsorbent (CAA), 0.8 g of 5-(2-chloroacetamide)-2-hydroxybenzoic acid was transferred into a round bottom flask containing 30 mL of toluene and then interacted with 1 g of amino aluminum powder at 130 °C for 24 h. The obtained CAA was filtered, washed several times with ethanol and dried at 50 °C for 6 h.

2.4. Theoretical computation for geometry and binding affinity

The structures of dibenzoylmethane, isatoic anhydride and 5-(2-chloroacetamide)-2-hydroxybenzoic acid were optimized using DFT to the minimum energy with the GGA/RPBE with DNP basis set.[25] All calculations were performed using the Material Studio platform *via* the DMOL^3 tool.[26,27] The chemical softness (S) and

hardness (η) reactivity indices were calculated using the energies of the HOMO and LUMO MO's using the following equations:[28]

$$\eta = \frac{1}{2}(E_{LUMO} - E_{HOMO})$$

$$S = \frac{1}{2}\eta$$

2.5. Extraction procedure

Different binding experiments were carried out to evaluate the binding ability of the constructed modified sorbents. All sorption experiments were performed depending on batch technique. At different pH values, a fixed dose of modified aluminum scrap (BAA or IAA or CAA) was suspended in 30 mL of various concentrations of target heavy metal ion (Hg(II) or Cd(II)) ranging from 50 mg L^{-1} to 300 mg L^{-1}. The mixtures were then kept shaking for different interval times (2–30 min) in a thermostatic shaker bath till an equilibrium was reached at 25 °C. After that, the supernatant was filtered with a porous membrane (pore size = 0.45 μm), and the equilibrium concentrations of the metal ions were detected by ICP-OES and FAAS. The percentage of heavy metal extract was calculated using the following equation;

$$\%\ R = \frac{(C_i - C_f)}{C_f} \times 100$$

where; C_i and C_f refer to the initial and final concentrations of the residual chemical ions (mg L^{-1}).

2.6. Application

2.6.1. Vegetable samples. Vegetable samples of cucumber were collected from a local market and were washed several times with tap water and rinsed three times with DDW. The samples were sliced into small parts and dried in an electrical oven at 80 °C for 4 hours. The dried samples were then crushed and homogenized with 100 mL of distilled water before digestion, then filtered through a porous membrane (pore size = 0.45 μm). After adjusting the pH value, the prepared samples were stored in a cool place and analyzed, followed by the extraction procedure outlined above.

2.6.2. Fish samples. Here, 0.5 g of dried fish muscle was mixed with 4 mL of conc. HNO_3–H_2O_2 (2 : 1 v/v), which was immediately prepared. The mixture was settled for 15 min at room temperature, then heated to near dryness and another amount of acid mixture was added. This step was repeated until the reddish-brown vapors stopped and a clear solution was obtained. The remaining sample was made up to 10 mL with DDW in a measuring flask, the pH was adjusted, and the total concentration of metal ions was determined according to the given extraction procedure.

2.6.3. Water samples. The water samples were collected from various places in Mansoura and Port-Said (Egypt). The samples were filtered through a cellulose membrane (0.45 μm) to remove any suspended materials. All samples were treated with HNO_3 and kept at pH 2 in the refrigerator in a dark polyethylene bottle.

3. Results and discussion

3.1. FT-IR

FT-IR spectra (Fig. 1) were utilized to clarify the modification of the aluminum scrap with different organic ligands. The aluminum spectrum is characterized by the presence of intense bands in the range 664–667 and 735–737 cm^{-1}, which are attributed to the symmetric and asymmetric stretching vibrations of Al–O–Al groups, respectively.[24] The bending vibrations of Al–O–Al groups were confirmed *via* the presence of a band in the range from 461 cm^{-1} to 465 cm^{-1}.[30] The bands that appeared at 1632 and 3424 cm^{-1} were assigned to the bending and stretching vibrations of OH groups, respectively.[29] New absorption bands were noticed for the BAA sorbent at 1641, 3000, and 3035 cm^{-1}, which refer to C=N stretching, and C–H stretching vibrations of aliphatic and aromatic structures, respectively. The presence of multiple bands in the region of 1449–1596 cm^{-1} confirmed the presence of aromatic C=C stretching vibrations. The presence of multiple bands in the 646–758 cm^{-1} region is due to aromatic CH out-of-plane bending vibrations. Moreover, the peak observed at 1346 cm^{-1} was due to the CH bending vibration. These results indicated the successful anchoring of dibenzoylmethane on the surface of the aluminum scrap. In the case of isatoic modification, FT-IR spectra showed a typical absorption peak at 1624 cm^{-1}, which was assigned to the C=N stretching vibration of the imine group. A novel band was shown in the region of 1442–1515 cm^{-1} that may be due to the existence of aromatic C=C stretching vibrations.[31] A sharp and strong peak was also seen at 1730 cm^{-1}, which may be due to the C=O stretching vibrations of the carbonyl group of the isatoic reagent. On the other hand, the spectra of CAA showed a sharp band at 3360 cm^{-1} that corresponds to the combination of N–H and

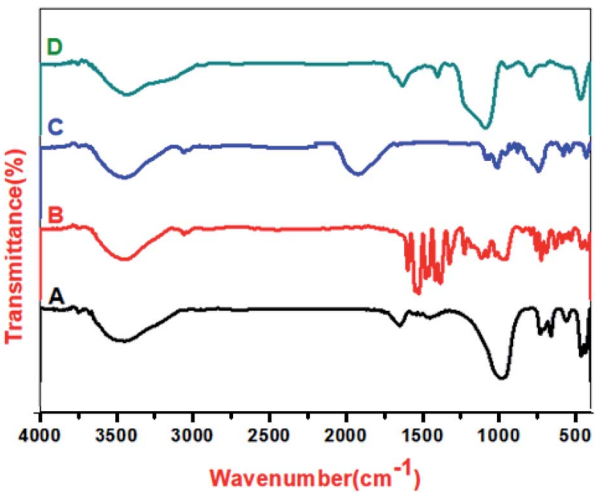

Fig. 1 FT-IR spectra of amino aluminum scrap (A), BAA (B), IAA (C), and CAA (D).

–OH groups.[32] Moreover, the bands that existed at 1750 cm^{-1}, 1539 cm^{-1}, and 782 cm^{-1} may be due to the stretching of the carboxyl group, C– H stretching of the aromatic backbone vibration, and aromatic C–H out-of-plane deformation of *ortho* disubstituted benzene, respectively.[33] Additionally, the peak at 1651 cm^{-1} was attributed to the absorbance of the symmetric stretching vibration of COO– of the new modifier, which confirmed the presence of 5-(2-chloroacetamide)-2-hydroxybenzoic acid at the surface of the modified sorbent.

3.2. SEM and XRD

The surface morphology and particle size of the modified sorbents were characterized by scanning electron microscopy, and the SEM patterns are shown in Fig. 2. The regular crystalline structure of mesoporous aluminum overlapped or combined over an amorphous background, relatively narrow size distribution, and good dispersibility were observed. Their particle sizes were nearly less than 100 nm and hence gave an expected high surface area. To confirm the crystallinity of BAA, IAA, and CAA, X-ray diffraction patterns of these sorbents are given in Fig. S1 (ESI).† The XRD spectra of mesoporous BAA showed a wide peak in the range of $2\theta = 15°–40°$. A broad peak centered at 2θ of 22.9° appeared with a wider *d*-spacing for aluminum scrap, which was modified with isatoic anhydride reagent. The crystallite size of the modified sample was calculated using the Debye–Scherrer equation and it was found to be 16.35 nm. On the other hand, the principal points of CAA were observed in the range $2\theta = 15°–40°$and the crystallite size was reduced to 13.2 nm. Therefore, it is important to report that the various chelating agents did not influence the crystal structure and morphology of the aluminum scrap.

3.3. Elemental analysis

The chemical composition of the constructed sorbents was elucidated by elemental analysis, and the obtained data are listed in Table 1. The appearance of nitrogen element in amino-aluminum scrap is a good indicator of the insertion of 3-aminopropyl trimethoxysilane during the chemical process. The enrichment in the percentages of carbon, hydrogen, and nitrogen after the modification with the different chelating ligands confirmed the completion of the modification processes.

Table 1 Elemental analysis of amino-Al, BAA, IAA, and CAA

Sample	C%	H%	N%
Amino-Al	8.68	1.98	1.62
BAA	13.25	3.22	2.78
IAA	17.34	2.54	3.66
CAA	18.12	4.13	4.23

3.4. Thermal gravimetric analysis (TGA)

As shown in the thermograms of the complexes in Fig. S2 (ESI),† the first degradation step occurred in the temperature range of 210–280 °C with small weight loss corresponding to the loss of water molecules. From the second to the last steps of degradation in the range of 280–800 °C were attributed to the decay of organic moieties of the coordinated ligand. The final remaining weights of metal complexes were 18.29%, 16.87%, 15.23%, 24.27%, 15.42% and 25.84% for Cd–BAA, Hg–BAA, Cd–CAA, Hg–CAA, Cd–IAA and Hg–IAA complexes, respectively. The high value of the remaining weight after the adsorption of the heavy metals indicates their higher thermal stabilities.

3.5. XPS analysis

XPS measurements were executed to elaborate on the chemical nature of adsorption of mercury and lead on the BAA surface. The XPS spectra before and after the adsorption of heavy metal ions at the surface of the sorbent are exhibited in Fig. S3 (ESI).† The main elements that were noted at the surface of BAA are Al, C, N, O, and Si, which demonstrated the successful preparation of the target sorbent. Furthermore, the appearance of cadmium and mercury peaks at 416.03 eV and 103.45 eV, respectively,

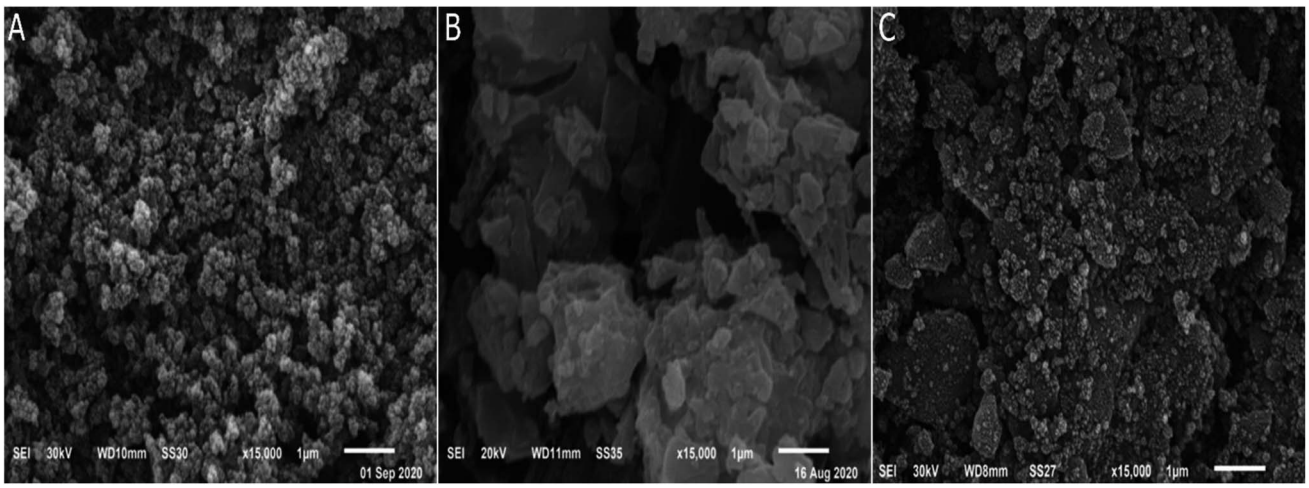

Fig. 2 Scanning electron micrographs of (A) BAA, (B) IAA, and (C) CAA.

emphasized the insertion of the target metal on the BAA surface. Also, the significant differences in intensities and peak positions of O 1s and N 1s before (532.45, and 400.45 eV for O 1s and N 1s) and after the adsorption of Hg(II) (534.6, and 400.6 eV for O 1s and N 1s) and Cd(II) (535.1, and 400.69 eV for O 1s and N 1s) confirmed the participation of nitrogen and oxygen-containing functional groups in the adsorption of metal ions.

3.6. Theoretical studies for the proposed chelating ligands

To verify the reactivity of complexation between the chelating ligands and the proposed heavy metals Hg(II), and Cd(II), the MEP maps (molecular electrostatic potential maps), frontier molecular orbitals (FMOs) and the reactivity indices were evaluated. Molecular orbitals (MOs) are significant in the qualitative analysis, in which different positioning is expected for the possibility of a reaction.The concept of FMOs is introduced when studying applications such as organometallic complexes, pericyclic reactions, and acidic–basic behavior.

Table 2 shows the E_{HOMO}, E_{LUMO} and reactivity indices (hardness 'η' and softness 'S'), for the proposed ligands. The soft species (acid or base) are ones with high polarizability, while the harder ones are less polarizable.[29] Based on this, it is concluded that the adsorption matrices for the different chelating ligands are soft ligands (gives values close to softness), being that the dibenzoylmethane is relatively softer than isatoic anhydride, which is softer than 5-(2-chloroacetamide)-2-hydroxybenzoic acid, as shown in Table 2. This is due to the existence of many regions that achieve resonance in ligands, such as the aromatic rings, along with the imine and carboxyl groups; this led to greater dispersion of the electrons on the ligand structures, producing an enhancement in the smoothness.

For the metal ions, the Hg^{2+} ions show the greatest softness while the Cd^{2+} ions give the highest hardness.[35] By considering Pearson's theory, which states that "the softer cations prefer interactions with the softer ligand while harder cations interact with harder ligands",[34] we conclude that Hg^{2+} ions have a greater tendency to interact with the ligands. On the other hand, the Cd^{2+} ions show the lowest ability for adsorption but since various ligands have relatively similar softness and hardness values, it can be deduced that mercury is the better metal for adsorption in these three ligands. Accordingly, dibenzoylmethane is the best adsorbent for Hg^{2+} adsorption.

The study of MEP maps is used in literature to locate the sites of interaction.[36] The FMOs and MEPs are represented in Fig. S4 (ESI).† For the MEP maps, the regions of intense blue color are the positive areas (E^{+} attack), and the regions of orange-red color are of more negative charge ($N^{\ddot{u}-}$ attack). From the MPEs, as seen in Fig. S4 (ESI),† it is possible to indicate that the metallic ions (positive ions) will interact with the oxygen and nitrogen atoms of the dibenzoylmethane ligand, which has more negative charges in the areas where the oxygen and nitrogen exist. In the case of isatoic and 5-(2-chloroacetamide)-2-hydroxybenzoic acid ligands, the MEP maps indicate the involvement of the oxygen atoms of both ligands in the interaction with metal ions. From the position of the FMOs (frontier molecular orbitals) for the dibenzoylmethane, as shown in Fig. 3, the position of HOMO orbitals indicates the coordination of the dibenzoylmethane ligand with the metal cations *via* the nitrogen atom of the (C=N) group, as the nitrogen atom grants π-orbitals that can interact with the metal cations, while in the case of isatoic and 5-(2-chloroacetamide)-2-hydroxybenzoic acid ligands, very distinguishing π-orbitals are located over the oxygen atom of the (C=O) groups so this would be the site of interaction for these ligands.

The chelating ligands use their HOMO level, which contains electrons, to interact with the empty LUMO levels of the electropositive Hg^{2+} and Cd^{2+} and species that have type-d orbitals.

3.7. Optimization of extraction conditions

3.7.1. The effect of pH. The pH was the first variable adjusted in the extraction process because it is a key parameter that regulates the extraction of metal ions. In the pH range of 3–8, the effect of pH was investigated and the data are presented in Fig. 4. The extraction efficiency of the chemical residual (Cd^{2+}, and Hg^{2+}) was sharply elevated with the increasing pH value by using differently prepared sorbents. The lower extraction efficiency of heavy metal ions was noticed in the acidic medium, which may be due to the protonation of the active sites of the ESI.† On increasing the pH values, higher recovery was achieved, which can be explained by the increased number of free sites formed at the adsorbent surface due to increasing the OH^{-} concentration resulting in the enhancement of the sorption rate. The maximum efficiency for the target metal ions was realized at pH 6 for Hg(II) and 5 for Cd(II). Also, the recovery percentages remained almost unchanged when the pH was elevated.

3.7.2. The effect of concentration. The adsorption capacity of the prepared sorbents was estimated by equilibrating 20 mg of each sorbent with 350 mL of the target heavy metal ion (50–300 mg L^{-1}) in capped conical flasks under the optimum pH conditions. Based on three replicate measurements, the experimental data were recorded in Fig. 5. As seen in the figure, the adsorption of the modified aluminum scrap decreased gradually with increasing the concentration of the target ions controlled by the driving force of mass transfer. After a definite

Table 2 FMO orbitals and the reactivity indices of hardness (η) and softness (S) for the ligands

Compound	E_{HOMO}	E_{LUMO}	Hardness (η)	Softness (S)
Dibenzoylmethane	−5.367542523	−2.164573934	1.601484	0.800742
Isatoic	−5.047153145	−1.977711876	1.534721	0.76736
Chloroacetamide	−5.275785008	−2.425886928	1.424949	0.712475

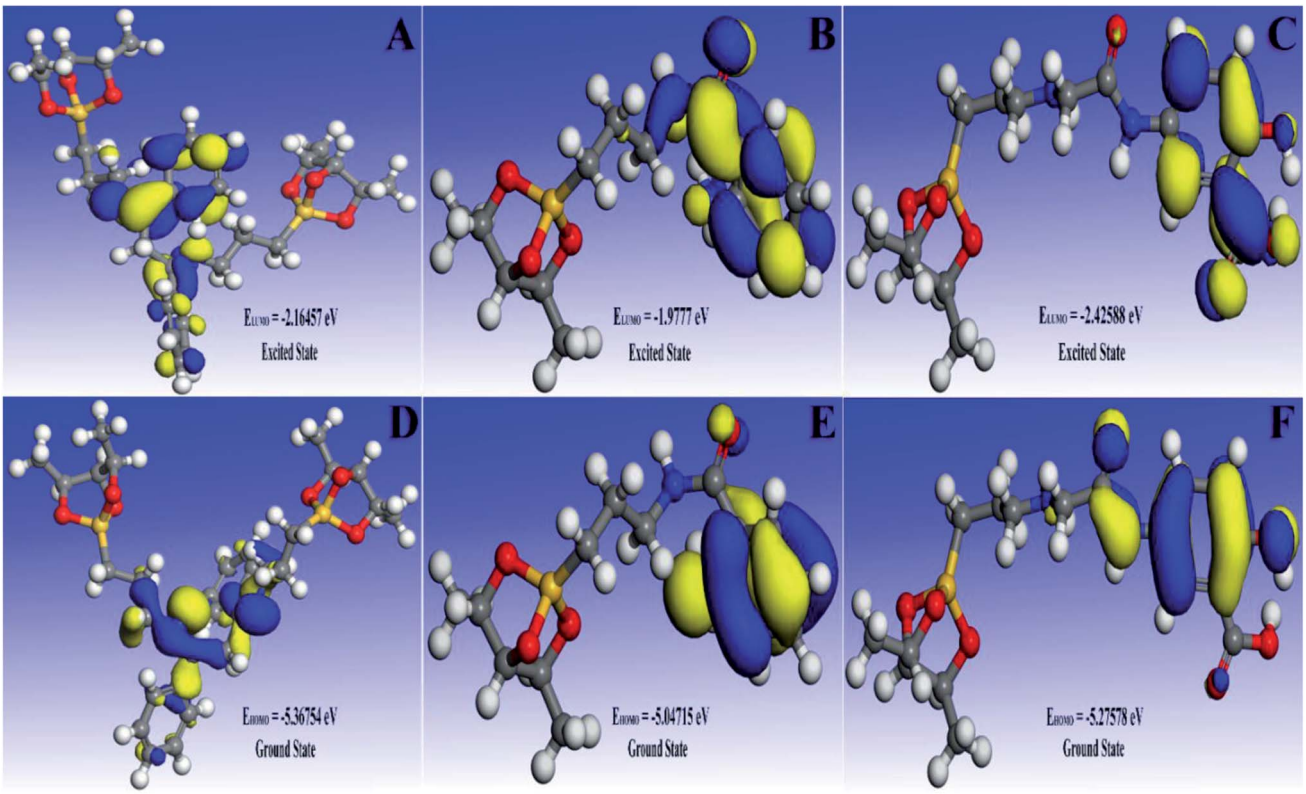

Fig. 3 (A–C) are HOMO orbitals for dibenzoylmethane, isatoic, and 5-(2-chloroacetamide)-2-hydroxybenzoic acid, respectively, and (D–F) are LUMO orbitals of dibenzoylmethane, isatoic, and 5-(2-chloroacetamide)-2-hydroxybenzoic acid, respectively.

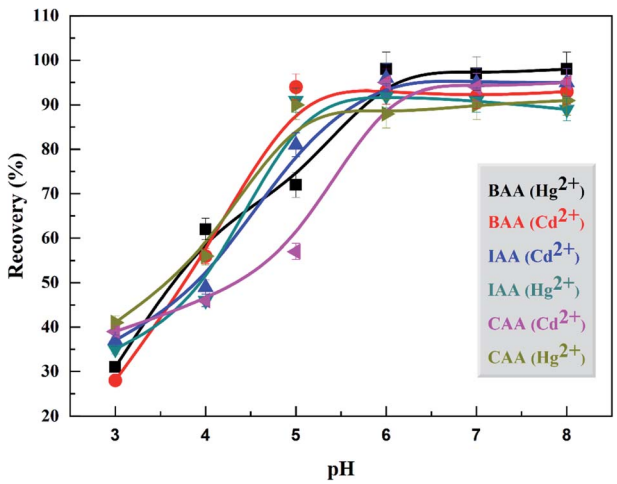

Fig. 4 The effect of pH on the extraction efficiency of Cd(II) and Hg(II) by using different modified sorbents (initial concentration 100 mg L^{-1}; contact time 5 min; temperature 298 K).

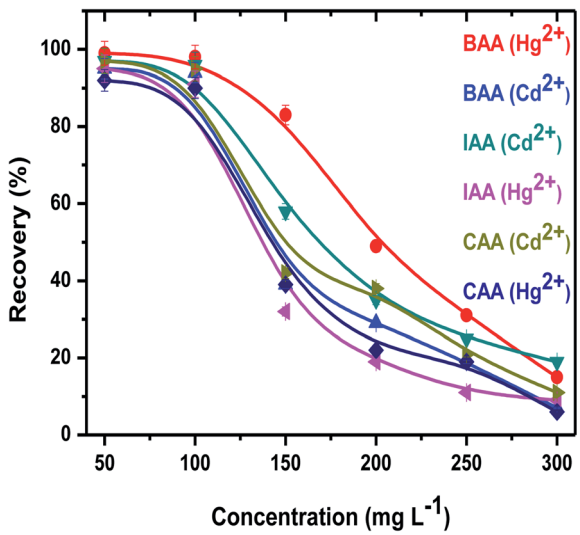

Fig. 5 The influence of the initial concentration of Cd(II) and Hg(II) on the extraction efficiency by using BAA, IAA, and CAA (pH 5 for Hg(II) and 6 for Cd(II); contact time 5 min; temperature 298 K; washing solvent HNO_3 (0.1 mol L^{-1})).

time, the adsorption recovery decreased with increasing its concentration due to its decreasing the number of active sites on the surface of ESI.† A high maximum percentage recovery of 98.6% was observed for Hg(II) by using BAA. The percentage recovery for cadmium was 91.3%. For IAA and CAA, the extraction recovery ranged from 85.3% to 88.6% for Cd(II), and from 92.3% to 94.1% for Hg(II).

3.7.3. The effect of contact time. The interval time required for complete extraction is a key factor in the efficiency of the assay. SoAs such, the extraction time was investigated by the batch system in the range of 2–30 min, while other parameters

were kept at optimum conditions. In a typical uptake kinetics test, 20 mg of the modified aluminum scrap was added to 10 mL of 10 mg L^{-1} of each heavy metal ion solution (Cd(II) or Hg(II)) at a specific pH and the resulting suspension was continuously stirred for various periods of time. After the adsorption stage, the supernatant solution was isolated and each heavy metal ion was detected with ICP-AES. As exhibited in Fig. 6, the extraction efficiency was rapidly elevated with increasing the shaking time and the complete recovery for each metal ion was achieved in less than 5 min. A monotonous increasing trend with high rates at the beginning of extraction may be attributed to the fact that there are a large number of vacant sites on the modified aluminum scrap. On increasing the contact time, the active vacant active sites became saturated and consequently, the adsorption rate decreased rapidly. To explore the interaction mechanism between the different modified aluminum scraps and each metal ion, the Lagergren pseudo-first-order and pseudo-second-order kinetic models were utilized to obtain the appropriate kinetic data. The linear expressions of the pseudo-first-order (eqn (1)) and second-order (eqn (2)) kinetic models for the extraction of each heavy metal ion are as follows:

$$\ln(Q_e - Q_t) = \ln Q_e - K_1 t \quad (1)$$

$$\frac{t}{Q_t} = \frac{1}{K_2 Q_e^2} + \frac{t}{Q_e} \quad (2)$$

where Q_e and Q_t are the adsorption quantities of heavy metals at equilibrium (mg g^{-1}) and any time (t). K_1 and K_2 (min^{-1}) are the rate constants of the pseudo-first and second-order reactions, respectively. As can be seen from Fig. S5 (ESI),† the sorption kinetics of heavy metals using various modified aluminum scraps were confirmed by the pseudo-second-order Lagergren equation, which has high correlation coefficients. Detailed data are shown in Table S1 (ESI),† which suggest that the adsorption process depends on the concentration of heavy metal ions and also the amount of the modified sorbent, favoring the covalent chemical bonds assumption.

3.7.4. Study of elution. The complete removal of adsorbed metal ions from the surface of synthesized modified aluminum scrap is a crucial step to guarantee the absence of memory effects. Therefore, various solvents such as nitric acid, hydrochloric acid, acetic acid, EDTA, and sodium hydroxide were explored to obtain the best eluent for the removal of the extracted ions. Compared with the other solvents, nitric acid showed excellent recovery. Moreover, the volume of nitric acid was checked to evaluate the preconcentration factor for these extraction processes. As listed in Table S2 (ESI),† quantitative recovery for each metal ion by different modified aluminum scraps was obtained with a lower volume of HNO_3 (0.1 mol L^{-1}) and subsequently higher preconcentration factors were noticed.

3.7.5. The effect of temperature. The uptake thermodynamics of the proposed metal ions on the surface of the modified sorbent was also investigated by using a static procedure. Thus, the extraction experiments were tested in the temperature range of 298–323 K. As exhibited in Fig. 7, higher adsorption capacities were observed after shaking for 4 min at 298 K in a water bath shaker. After the temperature exceeded 298 K, the capacity of the modified aluminum decreased, which may be attributed to the damage to different pores on the aluminum surface. Furthermore, the standard enthalpy change (ΔH°), standard Gibbs free energy change (ΔG°), and standard entropy change (ΔS°) were calculated, and the obtained data are presented in Table S3 (ESI).†[37] The negative values of free energy suggested that the adsorption reaction occurred spontaneously. The positive values of enthalpies and entropies indicate an endothermic and randomness interaction between the proposed metals and different modified sorbents.

3.7.6. The isotherm effect. Different isotherm models, including Langmuir and Freundlich, have been successfully utilized to fit the obtained experimental data. As can be seen

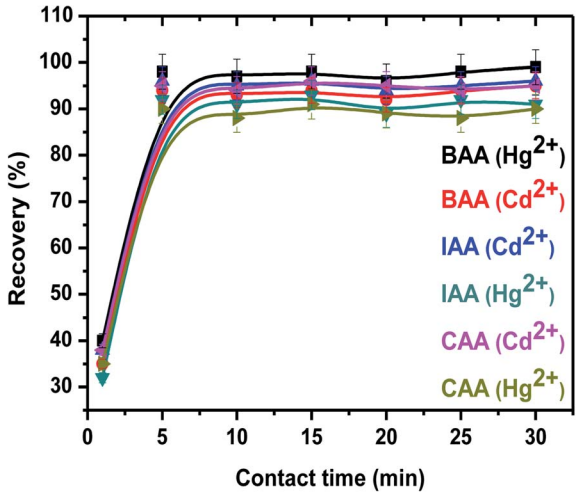

Fig. 6 The influence of contact time on the extraction efficiency of Cd(II) and Hg(II) by using different adsorbents (pH 5 for Hg(II) and 6 for Cd(II); initial concentration 100 mg L^{-1}; temperature 298 K; washing solvent HNO_3 (0.1 mol L^{-1})).

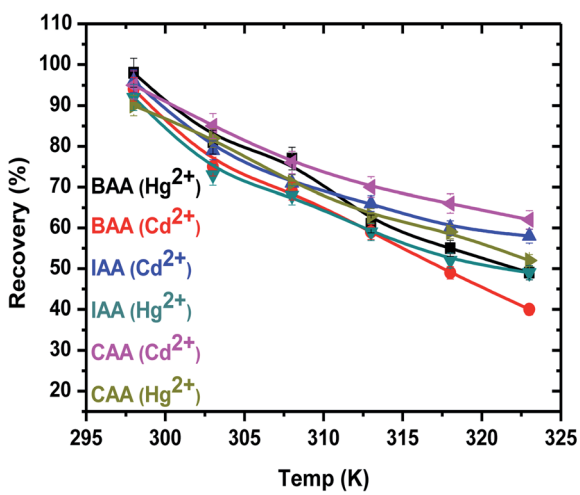

Fig. 7 The effect of temperature on the adsorption efficiency of Cd(II) and Hg(II) using BAA, IAA, and CAA. (pH 5 for Hg(II) and 6 for Cd(II); initial concentration 100 mg L^{-1}; contact time 5 min; washing solvent HNO_3 (0.1 mol L^{-1})).

Table 3 Recovery of Hg(II) and Cd(II) from different real samples (River Nile water, wastewater, seawater, fish muscle, and cucumber samples) by using the BAA, IAA, and CAA sorbents

		Found						Recovery (%)					
		BAA		IAA		CAA		BAA		IAA		CAA	
Sample	Amount added	Cd	Hg	Cd	Hg	Cd	Hg	Cd	Hg	Cd	Hg	Cd	Hg
River Nile water ($\mu g\ L^{-1}$)	—	0.12	0.35	0.1	0.33	0.11	0.31	—	—	—	—	—	—
	5.0	5.08	5.27	5.09	5.27	5.09	5.29	99.2	98.5	99.8	98.8	99.6	99.6
	10.0	10.1	10.31	10.08	10.31	10.12	10.18	99.8	99.6	99.8	99.8	100	98.7
Tap water ($\mu g\ L^{-1}$)	—	0.27	0.22	0.28	0.22	0.27	0.2	—	—	—	—	—	—
	5.0	5.15	5.13	5.17	5.2	5.24	5.22	97.7	98.2	97.9	99.6	99.4	100
	10.0	10.17	10.1	10.29	10.1	10.21	10.15	99	98.8	100	98.8	99.4	99.5
Seawater ($\mu g\ L^{-1}$)	—	0.22	0.29	0.21	0.27	0.22	0.26	—	—	—	—	—	—
	5.0	5.22	5.17	5.19	5.26	5.19	5.21	100	97.7	99.6	99.8	99.4	99
	10.0	10.21	10.11	10.1	10.27	10.1	10.1	99.9	98.2	98.9	100	98.8	98.4
Wastewater ($\mu g\ L^{-1}$)	—	0.56	4.12	0.55	4.1	0.57	4.2	—	—	—	—	—	—
	5.0	5.33	9.09	5.44	9.09	5.42	9.15	95.8	99.6	98	99.8	97.3	99.4
	10.0	10.5	14.1	10.42	14.1	10.36	14.2	99.4	99.8	98.7	100	98	100
Fish muscles ($\mu g\ L^{-1}$)	—	0.18	2.65	0.19	2.61	0.17	2.59	—	—	—	—	—	—
	5.0	5.07	7.51	5.18	7.49	5.16	7.48	97.8	98.1	99.8	98.4	99.8	98.5
	10.0	10.15	12.59	10.06	12.39	10.17	12.47	99.7	99.5	98.7	98.2	100	99
Cucumber ($\mu g\ L^{-1}$)	—	0.07	0.09	0.08	0.09	0.08	0.08	—	—	—	—	—	—
	5.0	5.03	5.01	5.06	5.09	5.0	4.97	99.2	98.4	99.6	100	98.4	97.8
	10.0	10.0	10.01	10.07	9.98	9.94	10.07	99.3	99.2	99.9	98.9	98.6	99.9

from Fig. S6 (ESI),† the Langmuir equation was more suitable for heavy metal extraction at the aluminum surface than the Freundlich equation. The maximum adsorption capacities were calculated and are listed in Table S4 (ESI).†

3.7.7. Interference effect. The efficiency of the proposed method for the selective monitoring of mercury and cadmium ions in the presence of other commonly coexisting ions was examined under optimized conditions. For this purpose, competitive adsorption of 0.02 mg L^{-1} of each target ion (Hg(II), and Cd(II)) and individually added interfering ions (*i.e.*, Co(II), Fe(III), Al(III), Ni(II), and Zn(II) in the concentration range of 0–100 mg L^{-1}) on the various modified sorbents was studied. After reaching adsorption equilibrium, the metal ions were detected by ICP-AES. The obtained results are summarized in Table S5 (ESI).† The highest recovery of the proposed metal ions by different modified aluminum scrap was observed, which indicated few significant effects by the interfering ions on the extraction process.

3.7.8. Analytical figure of merit. Under the optimized work conditions that have been selected, each modified aluminum scrap showed a wider linear calibration curve against different metal ion concentrations with a higher correlation coefficient (R^2) (Table S6).† Lower limits of detection (LOD) and limits of quantification (LOQ) were observed based on 3SD/*L* and 10SD/*L*, respectively, where SD is the standard deviation of the blank and *L* is the slope of the linear section of the calibration curve. Furthermore, acceptable reproducibility and intermediate precision were obtained with a relative standard deviation lower than 5%. The reusability of each modified aluminum scrap was estimated by monitoring the efficiency of nine batch samples for each target ion, separately. The extraction recovery of the prepared sorbents was still high, in the range of 94.2–97.5% of the first cycle, which confirmed the high stability of each adsorbent (Table S7, ESI†). Also, a higher enrichment factor (EF) was obtained for each aluminum scrap sorbent, which is based on the slope ratio of the calibration graph with and without preconcentration. The performance criteria of different modified aluminum scraps were compared with other sorbents in the literature for each target metal determination and the corresponding results are summarized in Table S8 (ESI).† High adsorption capacity, excellent stability and selectivity, and wider linear range were exhibited for our modified sorbent, all of which make great promising adsorbents for the selective extraction of Hg(II), and Cd(II).

3.7.9. Application. To verify the practical applicability and efficiency of the fabricated modified sorbents, the preconcentration of trace levels of target heavy metal ions was tested in water, fish, and vegetable samples. For the separation and extraction procedures, the pH of each real sample was adjusted and spiked with a certain amount of these metals. The recoveries were calculated by three parallel determinations depending on ICP-OES (Table 3). As can be seen, satisfactory results were obtained with recoveries ranging from 95.8% to 100% and the RSD values were lower than 5%. These results confirmed the feasibility of the fabricated modified aluminum scrap for measuring metal ions in different environmental and agricultural products.

4. Conclusion

Newly selective and sensitive sorbents were successfully synthesized by the modification of aluminum scrap with the different promising chelating agents including dibenzoylmethane, isatoic anhydride, and 5-(2-chloroacetamide)-2-

hydroxybenzoic acid. The fabricated sorbents were characterized by using IR spectroscopy, XRD, SEM, and elemental analysis. The theoretical and experimental adsorption studies revealed that the aluminum scrap modified with BAA is incredibly more selective for Hg(II) than Cd(II). Under the optimal conditions, the adsorption capacity of fabricated sorbents ranged from 135.28 mg g^{-1} to 229.3 mg g^{-1}, while reaching 234.56 mg g^{-1} in the case of the BAA ligand. In general, the proposed sorbents showed good chemical and physical stability over a wide pH range and can be utilized repetitively in more than six cycles without significant changes in properties. This extraction procedure offers acceptable precision, high accuracy, and a relatively low detection limit and can also be applied to detect low levels of Hg(II), and Cd(II) in different real samples.

Conflicts of interest

There are no conflicts to declare.

References

1 E. Sevigné-Itoiz, C. M. Gasol, J. Rieradevall and X. Gabarrell, *Resour., Conserv. Recycl.*, 2014, **89**, 94–103.
2 E. van der Harst, J. Potting and C. Kroeze, *Waste Manage.*, 2016, **48**, 565–583.
3 M. E. Grigore, *Recycling*, 2017, **2**(4), 24.
4 Z. Xin, *Colloids Surf.*, 2019, **567**, 205–212.
5 R. Sun, J. Zhao, Z. Li, J. Mo, Y. Pan and D. Luo, *Prog. Org. Coat.*, 2019, **133**, 77–84.
6 R. Sun, Z. Li, J. Zhao, J. Mo, Y. Pan and D. Luo, *Nano*, 2021, **16**, 2150133.
7 G. Guzzi, A. Ronchi and P. Pigatto, *Chemosphere*, 2021, **263**, 127990.
8 Z. Fu and S. Xi, *Toxicol. Mech. Methods*, 2020, **3**, 167–176.
9 V. Zarezade, M. Behbahani, F. Omidi, H. S. Abandansari and G. Hesam, *RSC Adv.*, 2016, **6**, 103499–103507.
10 S. Himeno, E. Kitano and K. Morishita, *Anal. Sci.*, 2007, **23**, 959–962.
11 J. Jiang, Z. Li, Y. Wang, X. Zhang, K. Yu, H. Zhang, J. Zhang, J. Gao, X. Liu, H. Zhang, W. Wu and N. Li, *Food Chem.*, 2020, **310**, 125824.
12 R. Sun, G. Ma, X. Duan and J. Sun, *Spectrochim. Acta, Part B*, 2018, **141**, 22–27.
13 M. Karve and R. V. Rajgor, *J. Hazard. Mater.*, 2007, **141**, 607–613.
14 Z. Zhu, S. Sun and X. Jing, *Chem. Pap.*, 2022, **76**, 401–408.
15 G. Yanyu, K. Jing, Y. Chenggen, Y. Qian and Z. Xu, *Chin. J. Org. Chem.*, 2020, **40**, 1760–1765.
16 Z. Zhu, W. Wang, F. Zhang and J. Liu, *Mater. Lett.*, 2020, **261**, 127011.
17 J. Zhang, K. Cao, X. Zhang and Q. Zhang, *Appl. Organomet. Chem.*, 2020, **34**, e5377.
18 X. Jing, C. Chen, X. Deng, X. Zhang, D. Wei and L. Yu, *Appl. Organomet. Chem.*, 2018, **32**, e4332.
19 E. L. Silva and P. d. S. Roldan, *J. Hazard. Mater.*, 2009, **161**, 142–147.
20 L. Wang, Y. Liu, Y. Liu, Y. Mao, J. Han, W. Li and Y. Wang, *Sep. Purif. Technol.*, 2021, **274**, 118917.
21 M. Shamsipur, M. Ramezani and M. Sadeghi, *Microchim. Acta*, 2009, **166**, 235–242.
22 M. Sajid, M. K. Nazal and I. Ihsanullah, *Anal. Chim. Acta*, 2021, **1141**, 246–262.
23 W. Aiming, *Crit. Rev. Environ. Sci. Technol.*, 2021, **51**, 44–112.
24 H.-L. Jiang, Q.-B. Fu, M.-L. Wang, J.-M. Lin and R.-S. Zhao, *Food Chem.*, 2021, **345**, 128841.
25 B. Hammer, L. B. Hansen and J. K. Nørskov, *Phys. Rev. B: Condens. Matter Mater. Phys.*, 1999, **59**, 7413.
26 B. Delley, *J. Chem. Phys.*, 2000, **113**, 7756–7764.
27 A. M. Younis, T. H. Rakha, M. M. El-Gamil and G. M. A. El-Reash, *J. Inorg. Organomet. Polym. Mater.*, 2022, **32**, 895–911.
28 R. G. Parr, in *Horizons of quantum chemistry*, Springer, 1980, pp. 5–15.
29 M. M. Hassanien, W. I. Mortada, I. M. Kenawy and H. El-Daly, *Appl. Spectrosc.*, 2017, **71**, 288–299.
30 X. Dai, F. Qiu, X. Zhou, Y. Long, W. Li and Y. Tu, *Electrochim. Acta*, 2014, **144**, 161–167.
31 Y. Wang, E. Wang, Z. Wu, H. Li, Z. Zhu, X. Zhu and Y. Dong, *Carbohydr. Polym.*, 2014, **101**, 517–523.
32 S. Deng, G. zhang, S. Chen, Y. Xue, Z. Du and P. Wang, *J. Mater. Chem. A*, 2016, **4**, 15851–15860.
33 E. Pretsch, P. Bühlmann, C. Affolter, E. Pretsch, P. Bhuhlmann and C. Affolter, *Structure determination of organic compounds*, Springer, 2000.
34 R. G. Pearson, *J. Am. Chem. Soc.*, 2002, **85**, 3533–3539.
35 I. H. S. Ribeiro, D. T. Reis and D. H. Pereira, *J. Mol. Model.*, 2019, **25**, 267.
36 A. M. Younis, T. H. Rakha, M. M. El-Gamil and G. M. A. El-Reash, *J. Mol. Struct.*, 2021, **1245**, 131110.
37 M. E. Khalifa, I. M. M. Kenawy, Y. G. Abou El-Reash and A. B. Abdallah, *J. Environ. Chem. Eng.*, 2017, **5**, 3447–3454.